

THIN DISCS, THICK DISCS AND TRANSITION ZONES

Guillaume Dubus¹

Abstract. Accretion onto a compact object must occur through a disc when the material has some initial angular momentum. Thin discs and the thicker *low radiative efficiency accretion flows* (LRAFs) are solutions to this problem that have been widely studied and applied. This is an introduction to these accretion flows within the context of X-ray binaries and cataclysmic variables.

Accretion describes the increase of the mass of an astrophysical object when matter is deposited onto it. The conversion of a fraction of the gravitational potential energy of the accreted material into radiation can dominate the emission from the system. Accretion is a major source of energy in a varied lot of astrophysical objects including interacting close binaries, active galactic nuclei and protostellar systems (the standard textbook is Frank et al. 2002).

My focus is on close binaries in which a normal star transfers mass onto a black hole/neutron star (X-ray binaries, XRBs) or white dwarf (cataclysmic variables, CVs) via Roche-lobe overflow. Exhaustive reviews of their observational properties may be found in Lewin et al. (1995) and Warner (1995) respectively. In these systems, an accretion disc forms around the compact object due to angular momentum conservation. The detailed characteristics of the flow depend upon how matter dissipates its potential energy and gets rid of its angular momentum in the disc. This basically leads to two extremes: the “low radiative efficiency” accretion flows (LRAFs, which are geometrically thick) and the radiatively efficient, geometrically thin discs (hence the title). This is an introduction to these solutions. §1 groups the basic tools needed to present the solutions in §2 (thin discs) and §3 (thick discs); §4 is a brief discussion of the transition from one to the other.

1 The building blocks

1.1 Accretion efficiency, Eddington luminosity

In Newtonian dynamics, the available gravitational energy from a small mass m moved from infinity to the surface R_* of the accretor is GM_*m/R_* . The energy

¹ California Institute of Technology, MC 130-33, Pasadena, CA 91125 gd@tapir.caltech.edu

released can be a sizeable fraction η of the rest-mass energy mc^2 when the accretor is a neutron star or black hole: assuming a thin disc and free fall at the innermost stable circular orbit then $\eta \approx 0.42$ for a maximally rotating Kerr black hole (Novikov & Thorne 1973; see also Gammie 1999).

The Eddington luminosity L_E is the luminosity for which radiation pressure exactly balances the gravitational pull on the accreted material. Accretion is quenched above this luminosity (but see Begelman 2001; Shaviv 2001). For a spherical inflow of ionised hydrogen such that the radiation pressure is due to Thomson scattering on electrons and the dominant gravitational pull is on the protons, L_E is:

$$\frac{GM_* m_p}{R^2} = \frac{L_E}{4\pi R^2} \frac{\sigma_T}{c} \quad \text{hence } L_E \approx 10^{38} (M_*/M_\odot) \text{ erg} \cdot \text{s}^{-1} \quad (1.1)$$

The luminosities of XRBs and CVs are generally lower than this limit (Lewin et al. 1995; Warner 1995). The Eddington mass accretion rate \dot{M}_E is defined as:

$$\eta \dot{M}_E c^2 = L_E \quad \text{i.e. } \dot{M}_E \approx 10^{18} (M_*/M_\odot)(0.1/\eta) \text{ g s}^{-1} \quad (1.2)$$

1.2 Accretion flow temperature

Assuming the gravitational energy is released into radiation at the surface of the compact object, the minimum temperature of the flow is that of the black body radiating the same luminosity. At the Eddington limit this gives:

$$4\pi R_*^2 \sigma T_{\text{bb}}^4 = L_E \quad \text{i.e. } kT_{\text{bb}} \approx 1.5 \text{ keV } (L_E/10^{38} \text{ erg s}^{-1})^{1/4} (R_*/10 \text{ km})^{-1/2} \quad (1.3)$$

Accreting black holes and neutron stars should radiate mainly in soft X-rays while white dwarfs ($R_* \approx 10^4$ km) should radiate in UV. This is consistent with observations (Lewin et al. 1995; Warner 1995).

On the other hand, the maximum temperature is obtained when all the gravitational potential energy is transformed into thermal energy e without radiation losses (adiabatic flow):

$$e = \frac{3}{2} \frac{kT_g}{\mu m_H} = \frac{GM_*}{R_*} \quad \text{i.e. } kT_g \approx 45 \text{ MeV } (M_*/M_\odot)(R_*/10 \text{ km})^{-1} \quad (1.4)$$

assuming ionised hydrogen ($\mu = 0.5$). This is twice the virial temperature of bound particles in circular orbit at R_* . Accretion onto a compact object can power the emission of gamma rays.

1.3 Disc formation

Matter infalling onto the compact object will generally have some non-zero angular momentum. A particle with a ballistic trajectory will therefore have $R^2\Omega = (R^2\Omega)_{t=0}$. At the radius of closest approach to the compact object $1/2(R\Omega)_c^2 = GM/R_c$ so that $2GMR_c = (R^2\Omega)_0^2$. Only a particle with very low angular momentum can directly hit the compact object ($R_c < R_*$). This condition is not

met in compact binaries where matter comes from an orbiting companion and the stream will go round the compact star and intersect itself. Subsequent shocks lead to the dispersion of energy and the stream settles onto a circular orbit with the initial angular momentum (see Lubow & Shu 1975 for details).

A steady supply of matter with some specific initial angular momentum piles up in a ring at this circularisation radius. There is no accretion unless some matter can transfer its angular momentum to reach smaller orbits. Under such a process, an accretion disc forms extending down to the compact object.

1.4 Angular momentum transport

One process by which particles may exchange angular momentum is viscosity (see e.g. Terquem 2001 for an introduction). In gas kinetic theory, molecular viscosity arises from the exchange of momentum across the surface of a fluid element. The resulting force is proportional to $\nu_{\text{mol}} \sim \lambda u$ where λ is the mean free path between collisions and u is the mean thermal speed of the particles. Assuming particles in a plasma interacting only via Coulomb forces leads to:

$$\begin{aligned}\lambda &\sim 1 \text{ cm } (T/10^5 \text{ K}) (\rho/10^{-8} \text{ g cm}^{-3}) \\ u &\sim 10^6 \text{ cm s}^{-1} (T/10^5 \text{ K})^{1/2}\end{aligned}$$

using typical accretion disc temperatures and densities (Frank et al. 2002). The viscosity coefficient is therefore $\nu_{\text{mol}} \sim 10^6 \text{ cm}^2 \text{ s}^{-1}$.

Anticipating a little bit on result from the thin disc model, we can get an order-of-magnitude observational estimate for viscosity in accretion discs. If the eruptions of dwarf novae, a sub-class of CVs (see §2.8), are due to the accretion of matter coming from the outer regions of a disc and transported by viscosity then $\nu_{\text{disc}} \sim R_{\text{d}} v_{\text{r}}$ where R_{d} is the outer disc radius and v_{r} is the radial velocity of the infalling matter. $v_{\text{r}} \sim R_{\text{d}}/\tau_{\text{e}}$ where τ_{e} is the timescale of the eruption. The disc radius can be estimated using e.g. the circularisation radius (§1.3) and typically will be $\sim 10^{10}$ cm. For an eruption lasting a day, $\nu_{\text{disc}} \sim 10^{15} \text{ cm}^2 \text{ s}^{-1}$ i.e. $\nu_{\text{disc}} \gg \nu_{\text{mol}}$. Molecular viscosity is much too weak to account for accretion in discs.

The process by which angular momentum is transported has been the subject of intense research with turbulent transport the prime suspect. Turbulent viscosity is often modelled using the Navier-Stokes formalism but with a coefficient $\nu_{\text{turb}} \sim \lambda_{\text{turb}} u_{\text{turb}}$ where the scale and speed are those of the turbulent eddies. These are dynamic properties of the fluid, not intrinsic as with molecular viscosity. In a disc, the size and speed of the eddies are likely to be limited by the scale-height H and sound speed c_{s} :

$$\nu = \alpha c_{\text{s}} H \tag{1.5}$$

where α is a parameter < 1 . This is the famous α parameterisation of disc viscosity first described in a landmark paper by Shakura & Sunyaev (1973). In the following I will use this parameterisation.

One would rather want to derive ν from first principles. At present, only turbulence arising from the magneto-rotational instability (MRI) has succeeded in predicting any significant viscosity (see Balbus & Hawley 1998 for a review). Fortunately, there is some sense in modelling the angular momentum transport and energy dissipation of MHD turbulence using the α parameterisation (Balbus & Papaloizou 1999). However, the mechanism may not work in weakly ionised flows and this is a problem for models with a cold accretion disc (Stepinski et al. 1993; Gammie & Menou 1998). Putative global hydrodynamical instabilities might take over in these conditions. There are other possibilities for angular momentum transport including instabilities in a self-gravitating disc (e.g. Balbus & Papaloizou 1999 and references therein), spiral waves excited by tidal torques (Spruit 1987), hydromagnetic winds launched from the disc (Blandford & Payne 1982), radiative viscosity (e.g. Loeb & Laor 1992) etc. However, these only apply in specific conditions.

1.5 Vertically integrated disc equations

The disc equations derive from the equations of fluid dynamics combined with a model for viscosity (which contains the turbulent magnetic field contributions in the MRI case), an equation of state for the gas and a description of the radiative processes. A standard set of assumptions to start with is:

- Axisymmetry so that $\partial/\partial\phi = 0$ in cylindrical coordinates.
- The only non-zero component of the stress tensor is the azimuthal shear $\tau_{r\phi}$.
- The gas is perfect so the internal energy per unit mass is $e = c_v T$ and the gas pressure $P = \rho e(\gamma - 1)$ with $\gamma = c_p/c_v$. Radiation pressure is neglected here for simplicity.

In addition I suppose the disc self-gravity is negligible (this assumption must be dropped for protostellar discs and AGNs) and that relativistic corrections are negligible (which is fine when more than a few gravitational radii away from the compact object). Assuming hydrostatic balance so that $v_z = 0$, the vertical momentum conservation is ($P = \rho c_s^2$):

$$\frac{\partial P}{\partial z} = -\rho g_z \quad \text{i.e.} \quad \frac{\partial \ln P}{\partial \ln z} = -\frac{\Omega_K^2}{c_s^2} z^2 \left[1 + \frac{z^2}{R^2}\right]^{-\frac{3}{2}} \quad (1.6)$$

If the height H from the midplane of the disc is $\lesssim R$ high order terms in z/R can be neglected. This equation can be integrated analytically for a perfect gas yielding $P(z)$ and $\rho(z)$. Averaging P over z gives a relationship between H and the mid-plane sound speed which, to a factor of order unity, is :

$$H = c_s/\Omega_K \quad (1.7)$$

The scale-height c_s/Ω_K appears in Eq. 1.6. The detailed vertical balance can be bypassed by assuming the disc height is given by this relationship. The Shakura-Sunyaev prescription for the viscosity becomes

$$\nu = \alpha c_s^2/\Omega_K \quad (1.8)$$

Note that ν is effectively integrated over z . With a Navier-Stokes formulation of the viscosity, the integrated stress is:

$$\tau_{r\phi} = \nu \Sigma R \frac{\partial \Omega}{\partial R}$$

where $\Sigma = 2\rho_o H$ is the column density and ρ_o is the mean density. The radial evolution equations are then integrated and decoupled from z , resulting in a set of time-dependent 1D equations:

$$\frac{\partial \Sigma}{\partial t} + \frac{1}{R} \frac{\partial}{\partial R} (\Sigma R v_r) = 0 \quad (1.9)$$

$$\frac{\partial v_r}{\partial t} + v_r \frac{\partial v_r}{\partial R} = R\Omega^2 - R\Omega_K^2 - \frac{1}{\rho_o} \frac{\partial P}{\partial R} \quad (1.10)$$

$$\frac{\partial R^2 \Omega}{\partial t} + v_r \frac{\partial R^2 \Omega}{\partial R} = \frac{1}{\Sigma R} \frac{\partial}{\partial R} (R^2 \tau_{r\phi}) = \frac{1}{\Sigma R} \frac{\partial}{\partial R} \left(\nu \Sigma R^3 \frac{\partial \Omega}{\partial R} \right) \quad (1.11)$$

$$T \frac{\partial s}{\partial t} + v_r T \frac{\partial s}{\partial R} = \frac{1}{\Sigma} (Q_{\text{vis}}^+ - Q_{\text{rad}}^-) \quad (1.12)$$

In order, we have the mass, radial momentum, angular momentum, and energy conservation equations. $R\Omega$ and v_r are the angular and radial velocities while $P = \rho_o c_s^2$. c_s and therefore T are the mid-plane values of the sound speed and temperature in this framework (Eq. 1.8). Again, only the dominant term in the radial component of gravity is kept $g_r \approx R\Omega_K$. In the thermal equation, s is the entropy and Q_{vis}^+ is the energy generated by the work of viscous forces in the annulus:

$$Q_{\text{vis}}^+ = \nu \Sigma \left(R \frac{\partial \Omega}{\partial R} \right)^2 \quad (1.13)$$

Q_{rad}^- represents radiative losses. Using $ds = de + Pd(1/\rho_o)$ the thermal equation can be rewritten as:

$$\frac{\partial e}{\partial t} + v_r \frac{\partial e}{\partial R} = -\frac{P}{\rho_o^2} \left[\frac{\partial \rho_o}{\partial t} + v_r \frac{\partial \rho_o}{\partial R} \right] + \frac{1}{\Sigma} (Q_{\text{vis}}^+ - Q_{\text{rad}}^-) \quad (1.14)$$

and e can be written using T_g (see Eq. 1.4):

$$e = \frac{c_s^2}{(\gamma - 1)} = \frac{T}{T_g} R^2 \Omega_K^2 \quad (1.15)$$

Other versions of these equations accommodate additional energy sources and sinks, conduction or convection terms, radiation pressure, different proton and electron temperatures, magnetic fields, relativistic corrections etc.

1.6 Steady state disc

A disc in steady state has $\frac{\partial}{\partial t} = 0$. Combining Eqs. 1.9 and 1.11 and integrating over R gives:

$$R^2 \Omega = \frac{\nu R^2}{v_r} \frac{\partial \Omega}{\partial R} + \text{constant} \quad (1.16)$$

Assuming there are no viscous torques at the surface of the compact object, the integration constant is $R_*^2 \Omega_*$. This term is very small compared to $R^2 \Omega$ far from the boundary layer. Writing $b = 1 - (R_*^2 \Omega_* / R^2 \Omega)$, Eq. 1.16 then gives

$$bv_r = \frac{\nu}{R} \frac{\partial \ln \Omega}{\partial \ln R} \quad (1.17)$$

The radial momentum equation can be rewritten using Eqs. 1.17 and 1.15 as:

$$\frac{\Omega^2}{\Omega_K^2} - 1 = (\gamma - 1) \left(\frac{T}{T_g} \right) \frac{\partial \ln P}{\partial \ln R} + (\gamma - 1)^2 \left(\frac{\alpha T}{b T_g} \right)^2 \left(\frac{\partial \ln \Omega}{\partial \ln R} \right)^2 \frac{\partial \ln v_r}{\partial \ln R} \quad (1.18)$$

Defining the cooling efficiency f as $1 - Q_{\text{rad}}^- / Q_{\text{vis}}^+$, the energy equation becomes:

$$fb \left(\frac{\Omega}{\Omega_K} \right)^2 \frac{\partial \ln \Omega}{\partial \ln R} = \left(\frac{T}{T_g} \right) \left[\frac{\partial \ln e}{\partial \ln R} - (\gamma - 1) \frac{\partial \ln \rho_o}{\partial \ln R} \right] \quad (1.19)$$

In a solution to the equations, f should be calculated self-consistently from the radiative processes. I find this set of dimensionless equations useful when discussing the assumptions that go into a thin or thick disc.

2 Radiatively efficient flows: thin discs

Thin accretion discs are flows in which the energy liberated by accretion is efficiently radiated locally. The next section (§3) deals with the LRAFs where this is not the case. Thin discs were first described by Pringle & Rees (1972) and Shakura & Sunyaev (1973). The standard presentation of this model may be found in the review by Pringle (1981, see also Frank et al. 2002).

2.1 Main properties in steady state

For a cool steady disc such that $T/T_g \ll 1$ then we must have $f \approx 0$ i.e. $Q_{\text{vis}}^+ \approx Q_{\text{rad}}^-$, viscous heating is balanced locally by radiative losses. In other words, the disc is radiatively efficient. The definition Eq. 1.15 of e as a function of T/T_g shows that $c_s \ll R\Omega_K$ hence

$$H/R \ll 1$$

A cool accretion flow is geometrically thin. It is easy to see from the dimensionless equations that $T/T_g \ll 1$ further implies that a steady flow is Keplerian with $\Omega \approx \Omega_K$, azimuthally supersonic with $v_\phi \approx R\Omega_K \gg c_s$ but that the radial inflow velocity

$$bv_r = -\frac{3}{2} \frac{\nu}{R} \ll c_s \quad (2.1)$$

is highly subsonic. The mass accretion rate in the disc, defined as

$$\dot{M} = -2\pi R \Sigma v_r \quad (2.2)$$

is a constant (Eq. 1.9). The balance of heating and cooling gives:

$$Q^+ = \frac{9}{4} \nu \Sigma \Omega_K^2 = Q^- = 2\sigma T_{\text{eff}}^4 \quad (2.3)$$

The factor 2 accounts for radiation losses from both sides of the disc. This can be rewritten using Eqs. 2.1-2.2 as

$$\sigma T_{\text{eff}}^4 = \frac{3b}{8\pi} \frac{GM_* \dot{M}}{R^3} \quad (2.4)$$

The disc dissipates an energy $3/2GM\dot{M}/R^2dR$ between R and $R + dR$ far from the inner boundary, three times more than the local release of gravitational energy. The extra energy comes from smaller radii with viscous transport redistributing the way the available gravitational energy is radiated in the thin disc. This equation also shows clearly that the emission of a *steady state* disc is independent of the particular heating mechanism (viscosity in this case). Thus, there is no need to know the local angular momentum transport mechanism in order to predict the disc luminosity.

Eclipse mapping has been used to test the radial dependence of the emission. In a high inclination system, the companion gradually eclipses different parts of the disc during its orbital motion. The resulting eclipse profile can be used to map the radial distribution of the disc brightness temperature. Results show that dwarf novae in outburst and persistent CVs (novae-like systems) have temperatures varying as $R^{-3/4}$ in agreement with expectations. On the other hand, quiescent dwarf novae show flat radial temperature distributions and that supports the disc instability model which is discussed later in §2.7 (not all observations fit this simple picture, see e.g. Smak 1994; Warner 1995; Baptista 2001).

2.2 Vertical structure

The thermal balance (Eq. 2.3) is written without any knowledge of the radiative processes that cool the disc. This is needed to relate Q_{rad}^- to the quantities appearing in the radial equations. For instance, one can solve for Q^- by integrating the hydrostatic balance (Eq. 1.6) and vertical radiative transfer equation (Eq. 1.12) explicitly. For optically thick radiation, this is like solving a stellar atmosphere (see Hubeny 1990, and references therein). The caveat is that additional assumptions have to be made on how viscous dissipation occurs locally in the layer (typically $q_{\text{vis}}^+ \propto P$).

The simple one zone model for the vertical structure has $H\Omega_K = c_s$, $\Sigma = 2\rho_0 H$, $\tau = \kappa\Sigma$ and $P = \rho_0 kT/\mu m_H$. The radiation pressure is neglected and κ is the Kramers opacity (Rosseland mean of bb, bf & ff processes). If the layer is optically thick, i.e. the disc cools at the maximum possible rate, the Eddington approximation for the radiative flux relates T_{eff} to T . These assumptions can be shown retrospectively to be valid for the range of densities and temperatures considered.

$$Q^- = \frac{4\sigma}{3\tau} T^4 = Q^+ = \frac{3}{8\pi} \frac{GM_* \dot{M}}{R^3} \quad (2.5)$$

This completes the set of equations and a steady solution can now be found (Frank et al. 2002):

$$\begin{aligned}
\Sigma &= 5.2 \alpha^{-4/5} \dot{M}_{16}^{7/10} M_1^{1/4} R_{10}^{-3/4} \text{ g cm}^{-2} \\
H/R &= 0.02 \alpha^{-1/10} \dot{M}_{16}^{3/20} M_1^{-3/8} R_{10}^{1/8} \\
T &= 14000 \alpha^{-1/5} \dot{M}_{16}^{3/10} M_1^{-1/4} R_{10}^{-3/4} \text{ K} \\
\tau &= 190 \alpha^{-4/5} \dot{M}_{16}^{1/5} \\
\nu &= 2 \cdot 10^{14} \alpha^{4/5} \dot{M}_{16}^{3/10} M_1^{-1/4} R_{10}^{3/4} \text{ cm}^2 \text{ s}^{-1} \\
v_r &= 3 \cdot 10^4 \alpha^{4/5} \dot{M}_{16}^{3/10} M_1^{-1/4} R_{10}^{-1/4} \text{ cm s}^{-1}
\end{aligned}$$

where M_1 is the mass of the compact object in solar units, R_{10} is the radius in units of 10^{10} cm and \dot{M}_{16} is the accretion rate in units of 10^{16} g s⁻¹. Around a black hole or neutron star the disc can extend down to small radii. As the temperature increases, electron scattering takes over from free-free as the major source of opacity. At very small radii and high accretion rates, radiation pressure can become dominant but the disc is then unstable (see §2.6).

2.3 Radiation spectrum

The outgoing spectrum of the optically-thick model is calculated by considering each disc annulus radiates as a blackbody at a temperature T_{eff} and integrating over R . The resulting spectrum is a modified disc blackbody (Fig. 20 of Frank et al. 2002). The maximum temperature of the radiation is reached close to the surface of the accreting object at $R = (7/6)^2 R_*$ (Eq. 2.4). σT_{eff}^4 is of the order of 1 eV in the case of white dwarfs, 10 eV for massive black holes and 1 keV for neutron stars and stellar mass black holes. The big blue bump in AGNs and the soft X-ray emission in X-ray binaries can be interpreted as modified blackbodies from a thin disc. Optical observations leave little doubt that thin discs are present in compact binaries (e.g. double-peaked emission lines, radial temperature profiles, statistics of eclipsing systems, orbital lightcurves etc).

But it was quickly recognized that these objects also show emission at higher energies, which cannot be explained by a thin disc (e.g. Lightman & Shapiro 1975). One possible origin for this radiation is the boundary layer where the angular velocity of matter decreases rapidly to match that of the compact object. Integrating Eq. 2.4 over R shows only half of the available energy $GM_*\dot{M}/R_*^2$ is radiated within the thin disc and the balance is dissipated in the boundary layer (when the object has a surface). Modelling the contribution of the boundary layer to the spectrum of CVs and neutron star XRBs is a difficult problem (see Regev 1991; Popham & Sunyaev 2001, and references therein). Other likely possibilities include contributions from a tenuous hot corona above the disc (somewhat analogous to the solar corona; see Poutanen 1998 and references therein) and/or emission from a different type of accretion flow closer to the compact object (see §2.6 and 3.2) and/or a jet (e.g. Markoff et al. 2001).

2.4 Evolving thin disc: timescales

A cool evolving disc is not necessarily Keplerian and this assumption must be made when studying time-dependent thin discs. Numerical simulations show this is a very good approximation (e.g. Ludwig & Meyer 1998). The radial momentum equation can be put in a dimensionless form:

$$\frac{v_r^2}{R^2 \Omega_K^2} \left(\frac{R}{v_r} \frac{\partial \ln v_r}{\partial t} + \frac{\partial \ln v_r}{\partial \ln R} \right) = \frac{\Omega^2}{\Omega_K^2} - 1 - (\gamma - 1) \left(\frac{T}{T_g} \right) \frac{\partial \ln P}{\partial \ln R} \approx 0 \quad (2.6)$$

showing $v_r \ll R\Omega_K$, just like the steady case. The conservation of angular momentum with $\Omega = \Omega_K$ leads to $v_r \sim \nu/R$ (see Eq. 1.17).

The major timescales of a thin disc are directly identified from the dimensionless forms of the other Eqs. 1.9-1.12. The dynamical timescale is:

$$t_{\text{dyn}} \sim \frac{R}{v_\phi} \sim \frac{1}{\Omega_K} \approx 100 \text{ s } M_1^{-1/2} R_{10}^{3/2} \quad (2.7)$$

This is the shortest timescale over which azimuthal inhomogeneities (e.g. flares) would be expected to vary. Assuming the typical scale for the radial variation is R , the angular momentum equation yields the viscous / accretion timescale:

$$t_{\text{vis}} \sim \frac{R^2}{\nu} \sim \left(\frac{T_g}{T} \right) t_{\text{dyn}} \approx 4 \text{ days } \alpha^{-4/5} \dot{M}_{16}^{3/10} M_1^{1/4} R_{10}^{5/4} \quad (2.8)$$

This is also the characteristic time R/v_r needed to accrete viscously matter initially at a radius R (see §2.5). This accretion timescale is much longer than the dynamical timescale. Perturbations to the hydrostatic balance propagate at the sound speed so the vertical timescale is:

$$t_{\text{vert}} \sim \frac{H}{c_s} \sim t_{\text{dyn}} \quad (2.9)$$

The characteristic time needed to establish hydrostatic balance is of the same order as the dynamical timescale i.e. short compared to the accretion timescale. The energy equation yields the thermal timescale:

$$t_{\text{ther}} \sim \frac{e}{q^+} \sim \frac{c_s^2}{\nu \Omega_K^2} \sim \frac{1}{\alpha} t_{\text{dyn}} \quad (2.10)$$

This is the characteristic timescale needed to establish the local balance of heating and cooling and is short compared to the accretion timescale.

2.5 Diffusion equation

The mass and angular momentum conservation equations of a thin disc, rewritten in terms of Σ , can be combined into a single evolution equation:

$$\frac{\partial \Sigma}{\partial t} = \frac{3}{R} \frac{\partial}{\partial R} \left[R^{1/2} \frac{\partial}{\partial R} \left(\nu \Sigma R^{1/2} \right) \right] \quad (2.11)$$

This diffusion equation describes how the column density Σ evolves from a given initial radial profile and is discussed in Lynden-Bell & Pringle (1974).

The most pedagogical example is that of an infinitely thin annulus of matter which spreads both in and out under the influence of a constant viscosity ν (Figs. 4-5 of Lynden-Bell & Pringle 1974). After an initial adjustment, the mass accretion rate onto the compact object approaches a self-similar regime where \dot{M} varies as some power of time t . This is characteristic of constant total angular momentum solutions. After a few viscous timescales $t_{\text{vis}} \sim R^2/\nu$, most of the initial mass is accreted onto the compact object while a decreasing fraction of the matter carries away the angular momentum at infinity. In a binary, the thin disc has an outer radius set by tidal torques and angular momentum is given back to the companion (Papaloizou & Pringle 1977). Semi-analytical solutions to this diffusion equation under different assumptions can also be found in e.g. Bath & Pringle (1981) and Lyubarskii & Shakura (1987).

2.6 Stability of steady thin discs

A steady thin disc is susceptible to thermal and viscous instabilities (Shakura & Sunyaev 1976; Pringle 1976). The first arises when cooling cannot keep up with heating i.e. if heating increases faster than cooling when the temperature of an annulus is raised (the thermal balance is local). The stability criterion is:

$$\left(\frac{\partial Q^+}{\partial T}\right)_{\Sigma} < \left(\frac{\partial Q^-}{\partial T}\right)_{\Sigma} \quad (2.12)$$

The thermal timescale is much shorter than the viscous timescale on which Σ evolves (§2.4). Setting Σ constant, $Q^+ \sim \nu\Sigma \sim T$ (Eq. 1.13). For optically thick radiative cooling then (Eq. 2.5) $Q^- \sim T^4/\tau \sim T^{15/2}H/\Sigma^2 \sim T^8$ (taking Kramers opacity $\tau \sim \rho_0 T^{-7/2}\Sigma$), hence the disc of §2.2 is thermally stable. However, if the medium is optically thin then $Q^- \sim H\rho_0^2 T^{1/2} \sim 1$ (again for free-free radiation) and the annulus is unstable (Pringle et al. 1973).

The disc is viscously unstable when perturbations of the density are amplified rather than smoothed out by accretion. The criterion for viscous stability is:

$$\frac{\partial \dot{M}}{\partial \Sigma} > 0 \quad \text{or} \quad \frac{\partial \nu \Sigma}{\partial \Sigma} > 0 \quad (2.13)$$

using $\dot{M} \sim \nu\Sigma$ (steady-state thin disc). The criterion is easily found by linearizing Eq. 2.11 for small perturbations. Density perturbations grow on the long viscous timescale so thermal equilibrium can be assumed. Since $Q^+ \sim \nu\Sigma\Omega_K^2 \sim PH\Omega_K$ and $Q^- \sim T^4/\kappa\Sigma \sim P/\Sigma$ one has $H \propto 1/\Sigma$ in a radiation pressure / electron scattering (κ constant) dominated annulus. Writing the hydrostatic equilibrium shows $P \sim (\Sigma/H)c_s^2 \sim \Sigma H\Omega_K^2 \propto 1$ is independent of Σ hence $\nu\Sigma \propto PH \propto 1/\Sigma$: the annulus is unstable to density perturbations (Lightman & Eardley 1974). This region is also thermally unstable (Sunyaev & Shakura 1975).

As mentioned in §2.2, the inner region of a steady thin disc at high \dot{M} is radiation pressure and electron scattering dominated. Hence the region from which

X-rays originate is unstable and much effort went into finding how to reconcile this fact with observations. The Shapiro-Lightman-Eardley (SLE) model is one such attempt in which the viscously unstable region gives way to a hot, optically thin plasma at small radii (Shapiro et al. 1976). In the SLE model, the protons are heated by viscous dissipation and cool by Coulomb interactions with electrons. The electrons lose their energy efficiently by local inverse Compton scattering on soft photons (explaining the observed hard X-rays) so they have a much lower temperature ($T_e \sim 10^8$ K) than the protons ($T_p \sim 10^{11}$ K). This solution is still thermally unstable (Pringle 1976). Lowering the temperature cools the flow back to the Shakura-Sunyaev solution. Raising the temperature increases viscous heating and decreases the inflow timescale so that protons do not have time to give their energy to the electrons before being accreted. Energy is advected and the SLE flow becomes a two temperature advection-dominated flow (see §3.2).

The conclusion that a radiation pressure dominated thin disc is unstable depends upon the assumptions made. The region can be stabilised by invoking a different viscosity law (Piran 1978), for instance one in which ν is proportional to the gas pressure only and not the total pressure (β viscosity). Other possibilities include e.g. mass depletion by a wind (Piran 1978) or irradiation heating from the boundary layer (Czerny et al. 1986). Most importantly, including radial advection of heat stabilizes the flow at higher accretion rates to give a *slim accretion disc* (see §3.2 below and Abramowicz et al. 1988).

2.7 The disc instability model

The stability of a disc can be studied by looking at the local thermal equilibrium curves. This is the set of (Σ, \dot{M}) such that $Q^+ = Q^-$ for given M_* , α and radius R in a steady-state disc. In steady-state, one can use indifferently T_{eff} or T_c instead of \dot{M} (Eq. 2.5). If $\partial\dot{M}/\partial\Sigma < 0$ somewhere along this curve then the annulus is unstable. This does not happen in the Kramers opacity regime (§2.6). But at temperatures lower than 10^4 K the opacity decreases dramatically due to hydrogen recombination. This reverses the slope of the (Σ, \dot{M}) relation until the temperature has dropped enough that hydrogen is neutral: there is a range of accretion rates for which the local annulus is unstable (Meyer & Meyer-Hofmeister 1981). Fig. 1 shows examples of thermal equilibrium curves calculated at several radii using a detailed vertical integration ($M_* = 7M_\odot$, $\alpha = 0.1$; the code is described in Hameury et al. 1998).

Such a curve, drawing an S in the (Σ, \dot{M}) plane, leads to a limit cycle (Bath & Pringle 1982). When mass transfer rates \dot{M}_t is in the unstable range, the annulus must either jump up on the top branch or down on the bottom branch. On the top branch the accretion rate is higher than the average \dot{M}_t so density decreases. When the density reaches Σ_{min} , a slight temperature perturbation causes the annulus to cool on a thermal timescale to the lower branch ($Q^- > Q^+$ in the region around Σ_{min}). The accretion rate is lower than \dot{M}_t on this branch so the density increases until Σ_{max} is reached, the annulus heats to the upper branch and the process repeats itself. Changes in Σ occur on the viscous timescale $t_{\text{vis}} \propto 1/T_c$ which

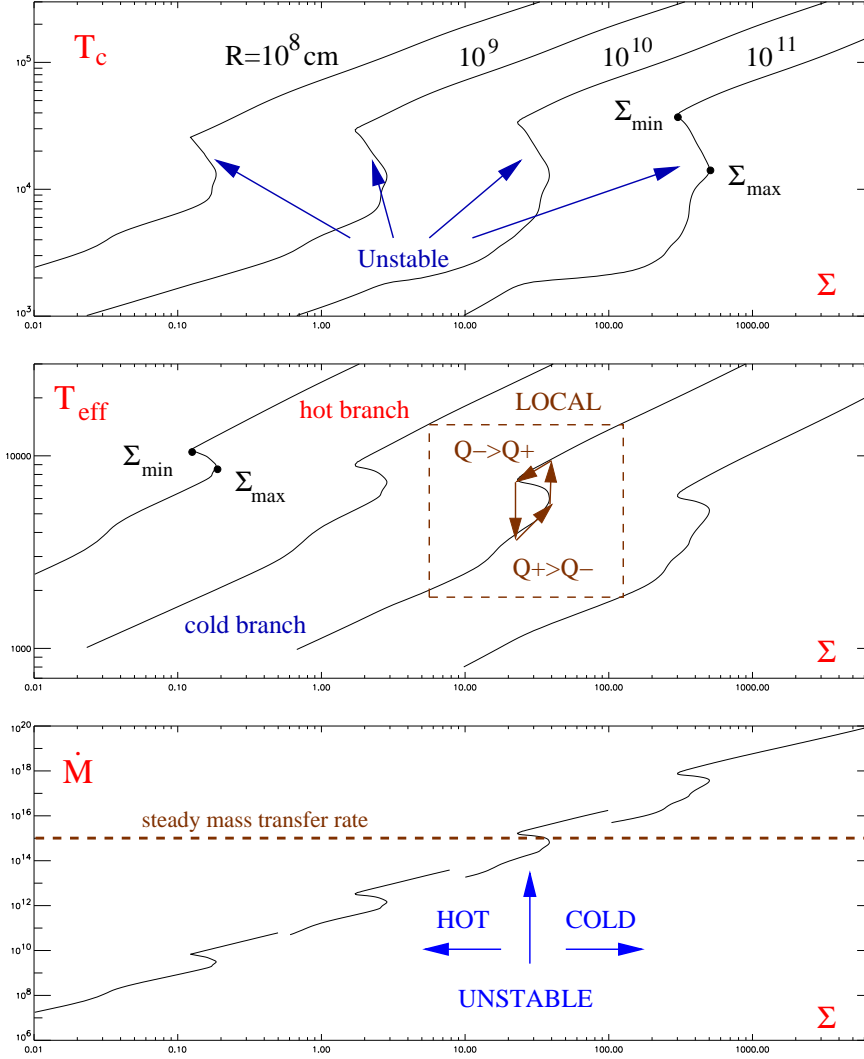


Fig. 1. Thermal equilibrium curves $Q^+ = Q^-$ calculated at different radii with $M_* = 7M_\odot$ and $\alpha = 0.1$. From top to bottom, the S curves are represented in the (Σ, T_c) , (Σ, T_{eff}) and (Σ, \dot{M}) planes (equivalent in steady-state). The middle branch is unstable due to hydrogen recombination and the local limit cycle is shown in the middle panel. For a large enough disc fuelled by a steady mass transfer rate the inner region is on the hot branch while the outer is on the cold branch (easily seen by looking at the intersection between the fixed \dot{M}_{rmt} and the S curves in the last panel). The intermediate region is unstable and numerical studies of the non-linear outcome show the disc cycles between a hot (outbursting) state and a cold (quiescent) state.

is shorter on the cold branch than on the hotter upper branch. The local cycle consists of a rapid rise to a brief high \dot{M} state followed by a longer low \dot{M} quiescent state. In a full disc the situation is complicated since mass is transferred from and to each region. The transitions in the (Σ, \dot{M}) plane are then more complex than the above picture suggests.

The critical values obtained from vertical structure calculations (Fig. 1) are well approximated by fits:

$$\begin{aligned}\Sigma_{\min} &\approx 8.3 \alpha^{-0.7} M_1^{-0.4} R_{10}^{1.1} \text{ g cm}^{-2} \\ \Sigma_{\max} &\approx 13.4 \alpha^{-0.8} M_1^{-0.4} R_{10}^{1.1} \text{ g cm}^{-2} \\ \dot{M}_{\Sigma_{\max}} &\approx 4 \cdot 10^{15} \alpha^{0.0} M_1^{-0.9} R_{10}^{2.7} \text{ g s}^{-1} \\ \dot{M}_{\Sigma_{\min}} &\approx 9 \cdot 10^{15} \alpha^{0.0} M_1^{-0.9} R_{10}^{2.7} \text{ g s}^{-1}\end{aligned}$$

For a steady disc to be everywhere on the hot branch (hence stable) requires $\dot{M}_t > \dot{M}_{\Sigma_{\min}}(R_{\text{disc}})$, giving values which are not unrealistic for XRBs and CVs. On the other hand, a stable steady *cold* disc requires $\dot{M}_t < \dot{M}_{\Sigma_{\max}}(R_*)$ which, due to the steep dependence on R , is very low: ~ 10 kg/s for a black hole/neutron star and $\leq 10^{13}$ g/s for a white dwarf. Cold, stable steady discs extending down to the surface of the compact object are unlikely to exist.

At intermediate accretion rates, the steady disc solution goes through the unstable branch at some radius. A density front appears and the disc evolves. The front speed is set by the radial inflow rate of matter (Eq. 1.11):

$$v_r = -\frac{3}{\Sigma R^{1/2}} \frac{\partial}{\partial R} (\nu \Sigma R^{1/2}) \quad \text{so} \quad v_f \approx \frac{\nu}{H} \approx \alpha c_s \quad (2.14)$$

since the typical scale of the variations is $\Delta R \sim H$. The propagation timescale is $t_f = R/v_f \sim (t_{\text{vis}} t_{\text{ther}})^{1/2}$, reflecting that this is a combination of the thermal and viscous instabilities. The disc enters a hot state until it cannot sustain the high accretion rate needed. A cooling front then propagates, shutting off accretion onto the central object and matter piles up until the cycle can start again.

This *disc instability model* (DIM) has been applied to CVs, XRBs, AGNs and protostellar discs (Hartmann & Kenyon 1996; Burderi et al. 1998; Lasota 2001). S curves have been calculated by many different groups using various assumptions and degrees of complexity for heat transport or viscous dissipation. Although it should really be confirmed from ab initio calculations of viscous transport, the reversal of the $\nu\Sigma$ slope is a robust unavoidable feature. The location of the critical Σ points can vary from model to model: this is equivalent to (small) variations in the unknown parameter α . But the critical accretion rates are independent of α as (a) H ionisation is what ultimately sets the critical (surface) T_{eff} so it is approximately constant (around 8000 K for the hot branch, see Fig. 1); and (b) \dot{M} is related to T_{eff} independently of ν (Eq. 2.4). Therefore, the essential feature of the DIM is a strong prediction of which systems should be stable. The second important aspect is that it offers a framework to understand the outbursts of unstable systems. In the following, I discuss the major results obtained from the application to cataclysmic variables and X-ray binaries (and defer to Lasota 2001, for a thorough review and complete references).

2.8 Models of Cataclysmic Variables

The DIM reproduces well the distinction between novae-like (steady) and dwarf novae (unsteady) systems for cataclysmic variables (Smak 1983; Osaki 1996). The DIM is also able to roughly reproduce the outbursts of dwarf novae (confirming the idea of Osaki 1974) but on one condition: that the viscosity on the hot branch is much higher than on the cold branch. Although ν varies with temperature, a constant α produces only small short outbursts because Σ_{\min} and Σ_{\max} are too close. To explain the amplitudes and timescales, α must change with $\alpha_{\text{hot}} \sim 0.1$ and $\alpha_{\text{cold}} \sim 0.01$ (Smak 1984). This is one of the most solid conclusions to come out of the DIM which can be tested against theoretical models of angular momentum transport. In the MRI case such a change is not inconceivable as its strength depends upon the gas ionisation fraction. Outbursts can therefore give some constraints on the viscosity, something steady state models cannot do.

However, further investigation shows that many additional effects need to be considered when modelling outbursts. For instance, the DIM assumes a steady mass transfer rate from the secondary but there is no reason for this to be the case. In fact, magnetic CVs do show variations of factors 10-100 which can be directly attributed to \dot{M}_t since they have no accretion discs. White dwarfs with lower magnetic moment can also disrupt the inner regions of a quiescent low \dot{M} disc. Tidal torques from the secondary are important in setting the outer disc radius, how it varies and determining the thermal balance in the outer regions. The impact of the stream of matter incoming from the Lagrange point and UV radiation from the hot white dwarf can also significantly heat the disc and change its properties (Buat-Ménard et al. 2001). A wide variety of CV lightcurves can be accounted for by varying combinations of these effects, using standard values for α and some earlier 'failures' of the DIM were actually due to missing some of these important phenomena (Lasota 2001).

However, there are still many unresolved issues and this testifies to large number of high-quality observations of CVs. For instance, the DIM cannot readily explain the flat quiescent lightcurves or some of the variations observed in the outbursts from cycle to cycle (Smak 2000). Moreover, the DIM still fails to make accurate spectral predictions, with fits requiring very large values of α . Oversimplification of the radiative transfer may be partly responsible but the issue really is that the vertical distribution of the heat generated by angular momentum transport is unknown. This has a major impact on spectral line formation. A related problem not addressed by the DIM is the formation of (line-driven) disc winds that can carry away sizeable fractions of the accreted matter.

2.9 Models of low mass X-ray binaries

Low mass X-ray binaries are very similar to CVs, with comparable companions, orbital periods and Roche lobe overflow mass transfer rates. One would therefore expect the DIM to work just as well as in CVs. But the standard DIM wrongly predicts that all observed systems should be transient. The solution to this prob-

lem is that one cannot neglect irradiation heating in X-ray binaries. High energy radiation coming from the inner regions of the flow can interact with the flow at larger radii and heat it to the upper branch of the S curve. A small fraction ($\sim 0.1\%$) of the luminosity deposited this way is enough to make a difference. Although there is ample evidence for irradiation in XRBs (Lewin et al. 1995), the geometry and processes through which high energy photons reach the outer disc are still unknown. They could involve a scattering corona, disc warps and/or a jet (as in the AGN lamppost model; Dubus et al. 1999).

A typical dwarf nova has eruptions lasting a few days and recurrence times of a few months. A typical transient XRB has an eruption lasting a few months with a recurrence period of years (Chen et al. 1997a). Since the main difference with CVs is not the mass of the accretor but its radius, one would think that the reason for the different outbursts has something to do with the flow reaching in to radii 10^{6-7} cm in XRBs instead of 10^{8-9} cm. But numerical simulations show such discs undergo large numbers of small amplitude, short duration and recurrence time outbursts. This is not surprising as Eq. 2.14 shows that the amount of mass needed to trigger an outburst (i.e. for $\Sigma > \Sigma_{\max}$) becomes very small at small R . Including irradiation in outburst lengthens the outbursts by keeping the disc hot longer but the models are still far from observed lightcurves. Another problem is that the accretion rate onto black hole has to be $\lesssim 10$ kg/s in quiescence since Σ must be lower than Σ_{\max} everywhere in the disc. But black hole XRBs are detected at levels of 10^{31} erg s $^{-1}$ which is incompatible with the accretion rate and the predicted $T_{\text{eff}} \approx 3000$ K in quiescent thin discs.

As it turns out, there is an elegant solution to *both* of these problems if the thin disc is assumed to be replaced ('evaporated') by a low radiative efficiency accretion flow (LRAF) at small radii in quiescence: (1) this removes the highly sensitive region which triggered many outbursts; (2) higher accretion rates can be 'hidden' in the radiatively inefficient flow and help increase the recurrence timescale (the disc acts as a pierced bucket trying to fill up); (3) spectral models of a class of such flows can explain the spectral energy distribution of quiescent XRBs. LRAFs are discussed in the next section.

Models of a modified DIM including irradiation and the evaporation of the inner thin disc show good agreement with the observed lightcurves (Dubus et al. 2001). These models do not require a different viscosity than that of CVs. This is gratifying since, after all, the conditions in the disc at large radii are not different in CVs and XRBs. On the other hand, the prospect of obtaining strong constraints on viscosity by comparing theoretical and observed lightcurves of CVs and XRBs fades away as increasingly complex (and poorly known) physics has to be added to the model.

3 Low radiative efficiency accretion flows: thick discs

The obvious contrast to the thin disc approach is to set $f \approx 1$ i.e. to look for solutions with little or no radiation cooling to Eqs. 1.9-1.6. The low radiative efficiency accretion flow (LRAF) obtained is cooled by the advection of viscous

heat (Ichimaru 1977; Katz 1977; Begelman 1978; Rees et al. 1982; Abramowicz et al. 1988; Narayan & Yi 1994, 1995b; Abramowicz et al. 1995). Being cooled by advection, LRAFs therefore have a radiative timescale which is longer than the accretion timescale: $t_{\text{acc}}/t_{\text{rad}} \sim (1-f)(R\Omega/c_s)^2 \ll 1$ when $f = 1$. Inversely, this ratio is very large (as expected) for the thin disc ($f = 0$) so there is a critical parameter value (e.g. \dot{M} at M_\star and α fixed), set by the detailed radiative processes, beyond which LRAFs can exist (see §3.2).

LRAFs are necessarily hot flows with $T \lesssim T_g$ (see Eqs. 1.18-1.19). A special case is that in which $f = 1$ and $\Omega = 0$ which corresponds to a purely radial accretion flow i.e. to the Bondi-Hoyle-Lyttleton solution describing accretion from the interstellar medium (Bondi & Hoyle 1944). In this sense, the adiabatic flows discussed below are a generalisation of this solution to the case of non-zero initial angular momentum.

Because of their high temperatures and low radiative efficiencies LRAFs provide an ideal context to model low luminosity objects showing emission at high energies (e.g. Lasota et al. 1996) and have thus attracted considerable interest. Since $T \lesssim T_g$ implies $H \lesssim R$, adiabatic flows are geometrically thick and more amenable to numerical simulations than thin discs in which radiation processes have to be taken into account and where resolving the very small vertical scale height is numerically challenging. Theoretical work on LRAFs has thus been enriched by the possibility to simulate adiabatic accretion, including ab initio transport of angular momentum via the MRI (hence requiring no additional assumptions).

The equations for a steady state accretion flow with an α type viscosity can be put in dimensionless form as shown in §1.6. Far from the boundary conditions, the equations have no length scale and a self-similar solution in which the variables are written in powers of R is possible. The thin disc is one special case with $f \ll 1$ and the next section describes the extension to arbitrary f (Spruit et al. 1987; Narayan & Yi 1994). In principle f is found self-consistently from the radiation transfer and this is done in a rudimentary way in §3.2, leading to the “unified description of accretion flows”. Some applications are presented in §3.3 while current problems and controversies in LRAFs are summarized in §3.4.

3.1 The self-similar solution

Assuming f is constant, Eqs. 1.18-1.19 immediately show that $\Omega \propto \Omega_K \propto R^{-3/2}$ and $T \propto T_g \propto R^{-1}$. Using these in Eq. 1.17 gives $v_r \propto R^{-1/2}$. The hydrostatic balance $H\Omega_K = c_s \propto T^{1/2}$ gives $H \propto R$, mass conservation gives $\Sigma \propto R^{-1/2}$ so $\rho_o \propto R^{-3/2}$. With these dependences, Eq. 1.18-1.19 solve for Ω and T from which the other variables can be deduced:

$$\Omega^2 = (\epsilon/f) h(\alpha, \gamma, f) \Omega_K^2 \quad (3.1)$$

$$v_r = -(3/2)\alpha h(\alpha, \gamma, f) R\Omega_K \quad (3.2)$$

$$T = (3/2)(1 + \epsilon) h(\alpha, \gamma, f) T_g \quad (3.3)$$

$$H/R = f/\epsilon \quad (3.4)$$

where $\epsilon = (5/3 - \gamma)/(\gamma - 1)$ and h is a function¹ of α , γ and f . To fix ideas, $\Omega \approx 0.7\Omega_K$, $v_r \approx 5 \cdot 10^7 \text{ cm}\cdot\text{s}^{-1}$, $T \approx 4 \cdot 10^9 \text{ K}$ and $H/R \approx 0.75$ at 10^9 cm around a $10 M_\odot$ black hole with $f = 0.75$, $\alpha = 0.1$ and $\gamma = 4/3$. The flow is sub-Keplerian, very hot and the accretion timescale is very short compared to the thin disc.

The thin disc is recovered as expected when $f \rightarrow 0$, giving $h \approx f/\epsilon \rightarrow 0$. In the other limit, as f increases towards 1, h increases so the temperature, viscosity and inflow velocity $v_r \sim \nu/R$ all increase. Since $t_{\text{acc}} = R/v_r \sim (1/h)t_{\text{ther}}$, the radial inflow time can become comparable to the thermal time. The disc becomes sub-Keplerian and thick with $H/R \lesssim 1$. If the gas is adiabatic with $\gamma = 5/3$, the flow becomes purely radial with $\Omega \rightarrow 0$ i.e. the solution tends to Bondi spherical accretion. Ogilvie (1999) studied the evolution of an initial torus of gas with some angular momentum at R accreting adiabatically, a setup similar to that described for thin discs in §2.5. He finds the self-similar solution with $f = 1$ is asymptotically approached with time.

There are some obvious limitations to the self-similar solutions. The self-similar solution extends at all R and does not address what happens at boundaries. But integration of the equations with physically motivated boundary conditions show the self-similar solution describes the flow well enough far from the boundaries (Chen et al. 1997b; Narayan et al. 1997). Global solutions to the equations in general relativity have also been found (Abramowicz et al. 1996; Peitz & Appl 1997; Popham & Gammie 1998). The validity of using the vertically integrated set of equations is not obvious when $H/R \sim 1$. Narayan & Yi (1995a) studied self-similar solutions to the equivalent 2D (R, θ) set of equations and found that the above solution was a good approximation if the integration is interpreted in terms of θ instead of z .

3.2 Radiative processes: ADAFs and slim discs

The parameter f was assumed given when it should really be found self-consistently from the radiative processes at all radii. In practice, this implies guessing f , determining Q^- for all relevant radiative processes (e.g. optically thick flux or free free, synchrotron, pair creation, comptonisation etc.) using the values for Σ and T from the radial solution, work out the improved value for f and repeat the process until convergence is reached (e.g. Narayan & Yi 1995b). To complicate things further there is no a priori reason for f to be constant in the flow but this is an assumption which is often made for simplicity and is likely to be reasonable in light of other approximations in the radiative transfer (Esin et al. 1997).

3.2.1 Optically thin case: ADAFs

Here, all of these complications are left aside and simple rudimentary forms for Q^- are used to find self-consistent solutions. The energy equation (Eq. 1.12) in

¹ $h(\alpha, \gamma, f)$ is the solution to $9\alpha^2 h^2 + 4(5 + 2\frac{\epsilon}{\gamma})h - 8 = 0$

steady state can be rewritten as (Abramowicz et al. 1995):

$$Q_{\text{adv}} = Q_{\text{vis}}^+ - Q^- \rightarrow \xi \left(\frac{\dot{M}}{2\pi} \right)^2 \frac{\Omega_K}{\alpha \Sigma R^2} = \Omega^2 \omega^2 \left(\frac{\dot{M}}{2\pi} \right) + \omega Q^- \quad (3.5)$$

where $\omega = d \ln \Omega / d \ln R$ and $\xi = d \ln \rho T^{1/1-\gamma} / d \ln R + 4(1-\beta) d \ln \rho T^{-3} / d \ln R$ for a mixture of perfect gas and radiation (β is the ratio of gas pressure to total pressure). In an adiabatic flow $Q^- = 0$ so the equation reduces to $\xi = \omega(R\Omega/c_s)^2$. Adiabatic accretion is possible for any \dot{M} when this is verified.

If Q^- is not negligible and the flow is emitting optically thin free-free radiation then $Q^- \sim H \rho_o^2 T^{1/2} \sim \Omega_K \Sigma^2$ ($\beta = 1$). For a given R , Σ and α the mass accretion rate \dot{M} satisfying the thermal equation (Eq. 3.5) depends on global properties of the flow. The thermal equation can be made local by assuming that the self-similar scalings hold and that $\Omega = \Omega_K$. Eq. 3.5 then becomes $\dot{M}^2 - \alpha C_1 \Sigma R^{1/2} \dot{M} + \alpha C_2 \Sigma^3 R^2 = 0$ (C_1, C_2 constants). Below a critical $\Sigma_{\text{crit}} \propto \alpha/R$ there are two possible solutions for \dot{M} : one with $Q^- > Q_{\text{adv}}$ corresponding to a Shapiro-Lightman-Eardley flow (see §2.6) and the other with $Q_{\text{adv}} > Q^-$ is called the advection-dominated accretion flow (ADAF) in the literature. Above the critical $\dot{M}_{\text{crit}} \propto \alpha^2 R^{-1/2}$ corresponding to Σ_{crit} there is no solution. \dot{M}_{crit} can also be found by equating the accretion timescale to the radiative timescale for bremsstrahlung: ADAFs appear when the latter becomes longer than the former.

3.2.2 Optically thick case: slim discs

In the optically thick case we have already seen that one solution is the Shakura-Sunyaev thin disc solution ($Q^+ = Q^-$). As \dot{M} increases, radiation pressure increases and the solution becomes unstable (§2.6). Writing the cooling term in the Eddington approximation with electron scattering opacity and assuming radiation pressure dominates, the thermal equilibrium can be rewritten with H/R instead of \dot{M} as:

$$Q_{\text{adv}} = Q_{\text{vis}}^+ - Q^- \rightarrow \xi \left(\frac{H}{R} \right)^3 = \left(\frac{H}{R} \right) \frac{\Omega^2}{\Omega_K^2} - \frac{C}{\alpha \omega R \Omega_K \Sigma} \quad (3.6)$$

where C is a constant. Again, this equation can be made local by assuming Keplerian rotation and ξ constant. For a given Σ , R and α there can be up to three solutions for H/R . Detailed calculations show an S-curve in the $(\Sigma, H/R)$ plane where the bottom branch is the Shakura-Sunyaev solution, the middle branch the unstable P_{rad} dominated thin disc and the top branch a new solution called the *slim disc* solution. Slim discs are radiation-pressure dominated and cooled by advection.

3.2.3 Thermal equilibrium curves

Both the ADAF and slim disc branches are thermally and viscously stable (see Honma et al. 1991; Kato et al. 1997, and references therein for details). An easy

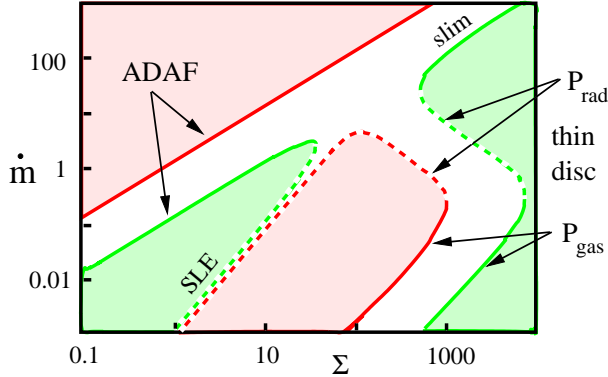


Fig. 2. A global view of the thermal equilibrium curves in the column density Σ , mass accretion rate \dot{m} (normalised to the Eddington rate) plane. This figure, adapted from Chen et al. (1995), shows the branches corresponding to different types of accretion. The curves are calculated at a radius of $30 R_g$ for a black hole of $10 M_\odot$ and using $\alpha = 0.1$ (green/light lines) or $\alpha = 1$ (red/dark lines). The dark areas enclose the regions where $Q^+ > Q^-$ in the case $\alpha = 0.1$ and $Q^- > Q^+$ in the case $\alpha = 1$. This shows the SLE solution (dotted lines) is thermally unstable in both cases (a slight increase in temperature at constant Σ pushes a disc on the SLE branch in the $Q^+ > Q^-$ region so that it cannot cool). On the other hand, the ADAF, slim disc and gas pressure dominated thin disc branches are stable. The radiation pressure dominated thin disc (dotted line) is thermally and viscously unstable.

way to see this is to plot the different branches found above in the (Σ, \dot{M}) in a similar fashion to what was done for the S-curves of the disc instability model in §2.7. This is shown in Fig. 2 (adapted from Chen et al. 1995). At low Σ , the disc is optically thin and there are two solutions: the thermally unstable SLE solution and the stable ADAF branch. At higher Σ , the disc is optically thick and there are three branches: the Shakura-Sunyaev thin disc (i.e. the upper branch of the S-curve in Fig. 1; the S corresponding to hydrogen ionisation occurs at much lower values of \dot{M} than shown in Fig. 2; see §2.7.), the radiation pressure dominated thermally/viscously unstable thin disc and the slim disc branch at high \dot{M} . There is a change of topology at a critical α above which an advection-dominated solution is possible for all \dot{M} . Although these curves are a useful tool to illustrate the various accretion solutions, it is worth stressing that they are local representations of an inherently non-local phenomenon (advection) and that they assume an α type viscosity. These curves therefore are not in any way a complete description of accretion flows.

3.3 Applications of LRAFs

LRAFs have applications to a variety of different objects in various situations. The S-curve at the transition between a thin disc and a slim disc (see Fig. 2), when

radiation pressure takes over, opens up the possibility of a thermal-viscous cycle like that described in §2.7. The associated mass accretion rates are very high and the timescales are very short so the cycle timescale is fast, of the order of seconds to minutes. This has found possible applications in some XRBs which accrete at high rates (e.g. Cannizzo 1996; Szuszkiewicz & Miller 2001, and references therein).

Optically thin LRAFs have many more applications. As mentioned at the end of §2, models of transient XRBs suggest a LRAF replaces the thin disc at small radii in quiescence. Support for this comes from models of optically thin LRAFs that reproduce the spectral energy distribution of quiescent X-ray binaries (Narayan et al. 1996). A comparison of the quiescent luminosities of neutron star transient XRBs against black hole transient XRBs shows that the neutron star systems are systematically more luminous by an order of magnitude or two than their black hole counterparts. This has been interpreted as evidence for a horizon in black holes. In both cases the compact object is surrounded by a LRAF. However, the energy stored in the flow is radiated when it reaches the surface of the neutron star while it disappears through the horizon in a black hole, explaining the luminosity difference (for a recent discussion see Garcia et al. 2001).

The Esin et al. (1997) model of transient XRBs spectral states is a natural extension of the idea that LRAFs and thin discs coexist. As the transient XRB goes into outburst, the ADAF retreats to smaller radii and eventually is fully replaced by the thin disc when the increasing mass flow rate is above the ADAF critical mass accretion rate (§3.2). Since the thin disc has a much lower temperature than the ADAF this roughly implies a transition between a hard and a soft X-ray spectrum during the rise to outburst and vice-versa during the return to quiescence. These ideas have been applied to the observed spectral changes in Nova Mus 1991 (Esin et al. 1997).

However, the most studied application of LRAFs is to Sgr A*, the black hole at the center of our Galaxy. Despite its dynamically-measured mass of a few $10^6 M_{\odot}$, the X-ray luminosity of Sgr A* is only 10^{33} ergs s^{-1} , well below the Eddington luminosity. The mass accretion rate inferred from observations is much higher than the luminosity suggests making it an ideal candidate for a LRAF. The dormant massive black holes at the center of nearby galaxies are also prime candidates for LRAFs (for a review of the above see Narayan 2002).

3.4 Current issues

3.4.1 LRAFs around neutron stars and white dwarfs

Matter accreting onto a black hole passes necessarily through the last marginally stable circular orbit and a sonic point before free-falling through the horizon. The inner boundary condition of global LRAF solutions around black holes is therefore provided by the regularity requirement at the sonic point. This sets the specific angular momentum accreted by the black hole. In contrast, matter falling onto a neutron star will have a vanishing radial velocity and may not necessarily pass through a sonic point (this depends on the neutron star radius i.e. equation of

state). The subsonic flow can spin-up or spin-down the neutron star. Energy released at the surface of the neutron star can significantly change the luminosity, spectra and heat budget of the accretion flow. All of these features make accretion onto a neutron star (or white dwarf) a difficult problem to tackle (see Medvedev & Narayan 2001, and references therein).

3.4.2 Two temperature plasmas

Optically thin LRAF solutions exist only below the critical mass accretion rate at which the accretion timescale is shorter than the radiation timescale (§3.2). Since it is mostly the electrons which radiate, this mass accretion rate is set by the electron temperature. To be astrophysically interesting, the electrons must be assumed to have a much lower temperature than the protons (Shapiro et al. 1976; Rees et al. 1982). This is achieved if viscous heating mostly goes to the protons and if these exchange heat with electrons only via Coulomb collisions (another issue is whether protons and electrons have enough time to thermalize before being accreted, see Mahadevan & Quataert 1997). All applications have assumed such two temperature LRAFs (the self-similar solution of §3.1 assumes a single temperature for simplicity). The relative fraction δ of heating that ultimately goes to the electrons depends on the microphysics and is uncertain (Narayan & Yi 1995b; Quataert 1998; Quataert & Gruzinov 1999). Plasma instabilities could erase any temperature difference between electrons and protons (Begelman & Chiueh 1988; Bisnovatyi-Kogan & Lovelace 1997). Observational constraints can in principle be obtained since the radiation spectrum depends on δ .

3.4.3 ADIOS

Another interesting feature appears when looking at the total local energy of the gas (per unit mass), defined as the sum of the kinetic, internal and potential energy from gravitation and pressure:

$$E = e_c + e_i + e_g + e_p = \frac{1}{2}(v_r^2 + R^2\Omega^2) + e - \frac{GM}{R} + \frac{P}{\rho} = \frac{3\epsilon(f - 1/3)}{5f + 2\epsilon} R^2\Omega_K^2 \quad (3.7)$$

This is also the Bernoulli integral, which is constant along streamlines for an adiabatic inviscid fluid ($\alpha=0$ and $f = 1$). Since the number is positive for $f > 1/3$, a particle going outwards on a streamline could reach infinity with a net positive energy, i.e. the fluid is energetically unbound and there could be an outflow. The local energy is positive because potential energy liberated at small radii is radiated at larger radii just like in the thin disc. When the flow cools efficiently this extra energy is efficiently radiated locally and the Bernoulli number is negative (which explains the $f = 1/3$ limit). Note that in the self-similar solution there is an infinite amount of energy released at $R = 0$ to redistribute hence it is unclear whether realistic boundary conditions will also yield a positive Bernoulli integral (Abramowicz et al. 2000).

The assumption that radiatively inefficient flows will necessarily lead to outflows is referred to as the Advection Dominated Inflow-Outflow Solution (ADIOS)

after Blandford & Begelman (1999). Work on ADIOS has focused on extensions of the ADAF with an outflow parameterised by $\dot{M} \propto R^p$ (p constant). Whether Nature prefers ADIOS to ADAFs is an open issue with no clear observational tests (Quataert & Narayan 1999) and conflicting numerical simulations (Hawley et al. 2001; Igumenshchev & Narayan 2002).

3.4.4 CDAF

It may turn out that neither ADAFs or ADIOS are correct descriptions. ADAFs are unstable according to the Hoiland criterion for convective stability of a rotating flow:

$$\text{stable if } (1 - \gamma) \frac{T}{T_g} \Omega_k^2 \left(\frac{d \ln P}{d \ln R} \right) \frac{d \ln(P^{1/\gamma}/\rho)}{d \ln R} + \Omega^2 \frac{d \ln(R^4 \Omega^2)}{d \ln R} > 0 \quad (3.8)$$

where the first term is the (squared) Brunt-Vaisala frequency (the frequency at which a perturbed blob of gas oscillates around its position in a stratified atmosphere) and the second term is the (squared) epicyclic frequency (the frequency at which a perturbed particle oscillates around its orbit). Convection will transport angular momentum and energy, changing the radial structure of the flow. The Convection Dominated Accretion Flow (CDAF) is one solution which assumes convection will transport angular momentum inwards (by analogy with axisymmetric hydrodynamic flows) and that the steady state flow is close to the marginally stable limit at which convective angular momentum transport balances outwards viscous transport. One condition for this to happen is that viscous transport is not too strong, i.e. for low values of α . There is then a net flux of energy outwards but very little net accretion (as opposed to ADAFs), yielding the CDAF self-similar scaling $\rho \propto R^{-1/2}$ (Narayan et al. 2000; Quataert & Gruzinov 2000). CDAFs have attracted a lot of attention because this density scaling was found in several numerical simulations (e.g. Stone et al. 1999). CDAFs are highly debated for several reasons: (1) purely hydrodynamical simulations with a Navier-Stokes viscosity may not catch the basic behaviour of a realistic flow; (2) MHD simulations may be inappropriate because the plasma is collisionless; (3) the Hoiland criterion may be inappropriate; (4) CDAFs may be thermodynamically impossible since energy dissipated in the MRI turbulent cascade cannot be used to generate convection (see e.g. Balbus & Hawley 2002; Hawley & Balbus 2002; Igumenshchev & Narayan 2002; Narayan et al. 2002).

4 The transition between thin and thick discs

As illustrated by Fig. 2, accretion with a given \dot{M} has a choice between several different types of flows. There is at present no guidance as to which particular type of flow is preferred, which admittedly an important open question when considering the potential applications of LRAFs. The flow may always prefer a LRAF whenever it is possible and this is called the strong LRAF (or ADAF) principle; or it may choose the LRAF only when there is no other solution available

(the weak principle). One application in which this has important consequences is the LRAF+thin disc model of transient XRBs. Insights into this issue might be gained by studying the directly related problem of the physics of the transition from a thin disc to a LRAF which is briefly discussed here.

4.1 Condition for the transition

Despite its shortcomings, an examination of Fig. 2 suffices to show most of the problems linked with the transition from a LRAF to a thin disc. A first possibility is to have a slim disc - thin disc transition but this occurs at high \dot{M} and there will be an unstable region (see §3.3). When $\alpha > \alpha_{\text{crit}}$ the thin disc makes a transition to the Shapiro-Lightman-Eardley type flow rather than the slim disc. However, the SLE flow is unstable (§2.6). These are the only possible smooth transitions with a thin disc and both will be unstable. The transition from a thin disc to an optically thin LRAF (ADAF), which is observationally motivated, necessarily involves some discontinuity in the framework of Fig. 2. At the transition, flow variables such as the radial inflow speed v_r or the temperature T must increase by several orders of magnitude and this involves some additional input of energy which is not taken into account in Fig. 2.

4.2 Possibilities

Studies of the transition between an optically thin LRAF and a thin disc therefore always involve some additional energy source. In the vertically averaged model of Honma (1996) the extra term comes from turbulent energy transport. This term dominates in the transition region. The transition is likely to be a 2D or 3D process that occurs gradually in radius i.e. the thin disc evaporates into a more tenuous gas in a sandwich around it. The study is therefore not much different from the studies of disc corona models. The generic idea is that radiative cooling is $\propto \rho^2$ so that any heating of the tenuous upper layers of a thin disc can lead to runaway heating (see §2.6) and from there to conditions reminiscent of LRAFs. The energy terms that can be involved include viscous heating (usually taken to be $\propto P$ hence $\propto \rho$, §2.6), heating by the reconnection of magnetic loops (Galeev et al. 1979), irradiation by photons or ions from the inner flow (Deufel & Spruit 2000), or electron conduction (Meyer et al. 2000, and references therein). Progress requires a better understanding of how the energy is dissipated, transported and radiated, much of which is based on difficult microphysics. This issue has started to be tackled by MHD numerical simulations (Miller & Stone 2000).

References

- Abramowicz, M. A., Chen, X., Kato, S., Lasota, J., & Regev, O. 1995, ApJ, 438, L37
- Abramowicz, M. A., Chen, X.-M., Granath, M., & Lasota, J.-P. 1996, ApJ, 471, 762

- Abramowicz, M. A., Czerny, B., Lasota, J. P., & Szuszkiewicz, E. 1988, *ApJ*, 332, 646
- Abramowicz, M. A., Lasota, J., & Igumenshchev, I. V. 2000, *MNRAS*, 314, 775
- Balbus, S. A. & Hawley, J. F. 1998, *Rev. Mod. Phys.*, 70, 1
- . 2002, *ApJ*, 573, in press
- Balbus, S. A. & Papaloizou, J. C. B. 1999, *ApJ*, 521, 650
- Baptista, R. 2001, in *Astrotomography, Indirect Imaging Methods in Observational Astronomy*, Ed. H.M.J. Boffin, D. Steeghs, J. Cuypers, *Lecture Notes in Physics*, vol. 573, 307
- Bath, G. T. & Pringle, J. E. 1981, *MNRAS*, 194, 967
- . 1982, *MNRAS*, 199, 267
- Begelman, M. C. 1978, *MNRAS*, 184, 53
- . 2001, *ApJ*, 551, 897
- Begelman, M. C. & Chiueh, T. 1988, *ApJ*, 332, 872
- Bisnovaty-Kogan, G. S. & Lovelace, R. V. E. 1997, *ApJ*, 486, L43
- Blandford, R. D. & Begelman, M. C. 1999, *MNRAS*, 303, L1
- Blandford, R. D. & Payne, D. G. 1982, *MNRAS*, 199, 883
- Bondi, H. & Hoyle, F. 1944, *MNRAS*, 104, 273
- Buat-Ménard, V., Hameury, J.-M., & Lasota, J.-P. 2001, *A&A*, 366, 612
- Burderi, L., King, A. R., & Szuszkiewicz, E. 1998, *ApJ*, 509, 85
- Cannizzo, J. K. 1996, *ApJ*, 466, L31
- Chen, W., Shrader, C. R., & Livio, M. 1997a, *ApJ*, 491, 312
- Chen, X., Abramowicz, M. A., & Lasota, J. 1997b, *ApJ*, 476, 61
- Chen, X., Abramowicz, M. A., Lasota, J., Narayan, R., & Yi, I. 1995, *ApJ*, 443, L61
- Czerny, B., Czerny, M., & Grindlay, J. E. 1986, *ApJ*, 311, 241
- Deufel, B. & Spruit, H. C. 2000, *A&A*, 362, 1
- Dubus, G., Hameury, J.-M., & Lasota, J.-P. 2001, *A&A*, 373, 251
- Dubus, G., Lasota, J., Hameury, J., & Charles, P. 1999, *MNRAS*, 303, 139

- Esin, A. A., McClintock, J. E., & Narayan, R. 1997, *ApJ*, 489, 865
- Frank, J., King, A., & Raine, D. 2002, *Accretion Power in Astrophysics*, 3rd ed. (Cambridge University Press)
- Galeev, A. A., Rosner, R., & Vaiana, G. S. 1979, *ApJ*, 229, 318
- Gammie, C. F. 1999, *ApJ*, 522, L57
- Gammie, C. F. & Menou, K. 1998, *ApJ*, 492, L75
- Garcia, M. R., McClintock, J. E., Narayan, R., et al. 2001, *ApJ*, 553, L47
- Hameury, J., Menou, K., Dubus, G., Lasota, J., & Hure, J. 1998, *MNRAS*, 298, 1048
- Hartmann, L. & Kenyon, S. J. 1996, *ARA&A*, 34, 207
- Hawley, J. F. & Balbus, S. A. 2002, *ApJ* in press (astro-ph/02033309)
- Hawley, J. F., Balbus, S. A., & Stone, J. M. 2001, *ApJ*, 554, L49
- Honma, F. 1996, *PASJ*, 48, 77
- Honma, F., Kato, S., Matsumoto, R., & Abramowicz, M. A. 1991, *PASJ*, 43, 261
- Hubeny, I. 1990, *ApJ*, 351, 632
- Ichimaru, S. 1977, *ApJ*, 214, 840
- Igumenshchev, I. V. & Narayan, R. 2002, *ApJ*, 566, 137
- Kato, S., Yamasaki, T., Abramowicz, M. A., & Chen, X. 1997, *PASJ*, 49, 221
- Katz, J. I. 1977, *ApJ*, 215, 265
- Lasota, J.-P. 2001, *New Astronomy Review*, 45, 449
- Lasota, J.-P., Abramowicz, M. A., Chen, X., et al. 1996, *ApJ*, 462, 142
- Lewin, W. H. G., van Paradijs, J., & van den Heuvel, E. P. J. 1995, *X-ray binaries* (Cambridge University Press)
- Lightman, A. P. & Eardley, D. M. 1974, *ApJ*, 187, L1
- Lightman, A. P. & Shapiro, S. L. 1975, *ApJ*, 198, L73
- Loeb, A. & Laor, A. 1992, *ApJ*, 384, 115
- Lubow, S. H. & Shu, F. H. 1975, *ApJ*, 198, 383
- Ludwig, K. & Meyer, F. 1998, *A&A*, 329, 559
- Lynden-Bell, D. & Pringle, J. E. 1974, *MNRAS*, 168, 603

- Lyubarskii, Y. E. & Shakura, N. I. 1987, *Soviet Astronomy Letters*, 13, 386
- Mahadevan, R. & Quataert, E. 1997, *ApJ*, 490, 605
- Markoff, S., Falcke, H., & Fender, R. 2001, *A&A*, 372, L25
- Medvedev, M. V. & Narayan, R. 2001, *ApJ*, 554, 1255
- Meyer, F., Liu, B. F., & Meyer-Hofmeister, E. 2000, *A&A*, 361, 175
- Meyer, F. & Meyer-Hofmeister, E. 1981, *A&A*, 104, L10
- Miller, K. A. & Stone, J. M. 2000, *ApJ*, 534, 398
- Narayan, R. 2002, in *Lighthouses of the Universe*, ed. M. Gilfanov, R. Sunyaev et al. (Springer-Verlag), (astro-ph/02011260)
- Narayan, R., Igumenshchev, I. V., & Abramowicz, M. A. 2000, *ApJ*, 539, 798
- Narayan, R., Kato, S., & Honma, F. 1997, *ApJ*, 476, 49
- Narayan, R., McClintock, J. E., & Yi, I. 1996, *ApJ*, 457, 821+
- Narayan, R., Quataert, E., Igumenshchev, I. V., & Abramowicz, M. A. 2002, *ApJ*, submitted (astro-ph/02033026),
- Narayan, R. & Yi, I. 1994, *ApJ*, 428, L13
- . 1995a, *ApJ*, 444, 231
- . 1995b, *ApJ*, 452, 710
- Novikov, I. D. & Thorne, K. S. 1973, in *Black Holes*, ed. C. DeWitt & B. DeWitt (New York: Gordon & Breach), 334
- Ogilvie, G. I. 1999, *MNRAS*, 306, L9
- Osaki, Y. 1974, *PASJ*, 26, 429
- . 1996, *PASP*, 108, 39
- Papaloizou, J. & Pringle, J. E. 1977, *MNRAS*, 181, 441
- Peitz, J. & Appl, S. 1997, *MNRAS*, 286, 681
- Piran, T. 1978, *ApJ*, 221, 652
- Popham, R. & Gammie, C. F. 1998, *ApJ*, 504, 419
- Popham, R. & Sunyaev, R. 2001, *ApJ*, 547, 355
- Poutanen, J. 1998, in *Theory of Black Hole Accretion Disks*, ed. M. Abramowicz, G. Bjornsson, & J. Pringle (Cambridge University Press), 100

- Pringle, J. E. 1976, *MNRAS*, 177, 65
- . 1981, *ARA&A*, 19, 137
- Pringle, J. E. & Rees, M. J. 1972, *A&A*, 21, 1
- Pringle, J. E., Rees, M. J., & Pacholczyk, A. G. 1973, *A&A*, 29, 179
- Quataert, E. 1998, *ApJ*, 500, 978
- Quataert, E. & Gruzinov, A. 1999, *ApJ*, 520, 248
- . 2000, *ApJ*, 539, 809
- Quataert, E. & Narayan, R. 1999, *ApJ*, 520, 298
- Rees, M. J., Phinney, E. S., Begelman, M. C., & Blandford, R. D. 1982, *Nature*, 295, 17
- Regev, O. 1991, in *Structure and Emission Properties of Accretion Disks*, IAU Colloq. 129, ed. J.-P. L. C. Bertout, S. Collin-Souffrin (Editions Frontieres), 311
- Shakura, N. I. & Sunyaev, R. A. 1973, *A&A*, 24, 337
- . 1976, *MNRAS*, 175, 613
- Shapiro, S. L., Lightman, A. P., & Eardley, D. M. 1976, *ApJ*, 204, 187
- Shaviv, N. J. 2001, *MNRAS*, 326, 126
- Smak, J. 1983, *ApJ*, 272, 234
- . 1984, *Acta Astronomica*, 34, 161
- . 1994, *Acta Astronomica*, 44, 265
- . 2000, *New Astronomy Review*, 44, 171
- Spruit, H. C. 1987, *A&A*, 184, 173
- Spruit, H. C., Matsuda, T., Inoue, M., & Sawada, K. 1987, *MNRAS*, 229, 517
- Stepinski, T. F., Reyes-Ruiz, M., & Vanhala, H. A. T. 1993, *Icarus*, 106, 77
- Stone, J. M., Pringle, J. E., & Begelman, M. C. 1999, *MNRAS*, 310, 1002
- Sunyaev, R. A. & Shakura, N. I. 1975, *Soviet Astronomy Letters*, 1, 158
- Szuskiewicz, E. & Miller, J. C. 2001, *MNRAS*, 328, 36
- Terquem, C. 2001, in *Proceedings of the Aussois 2000 Summer School on Star formation and the Physics of Young Stars*, ed. J. Bouvier & J.-P. Zahn (astro-ph/0107408)
- Warner, B. 1995, *Cataclysmic variable stars* (Cambridge University Press)